

# Rational Design, Green Synthesis, and Initial Evaluation of a Series of Full-Color Tunable Fluorescent Dyes Enabled by the Copper-Catalyzed N-Arylation of 6-Phenyl Pyridazinones and Their Application in Cell Imaging

Lei Liang,<sup>[a]</sup> Wei Wang,<sup>[a]</sup> Jun Wu,<sup>[b]</sup> Fengrong Xu,<sup>[a]</sup> Yan Niu,<sup>[a]</sup> Bo Xu,<sup>\*,[b]</sup> and Ping Xu<sup>\*,[a]</sup>

**Abstract:** There is widespread interest in the application, optimization, and evolution of the transition-metal-catalyzed arylation of N-heteroarenes to discover full-color tunable fluorescent core frameworks. Inspired by the versatile roles of pyridazinone in organic synthesis and medicinal chemistry, herein, we report a simple and efficient copper-catalyzed cross-coupling reaction for the N-functionalization of pyridazinones in neat water. To achieve the efficient conversion of pyridazinones and organic halides in aqueous phase, a series of copper-salen complexes composed of different Schiff base ligands

were investigated by rational design. A final choice of fine-tuned hydrophilicity balanced with lipophilicity among the candidates was confirmed, which affords excellent activity towards the reaction of a wide range of pyridazinones and organic halides. More importantly, the products as N-substituted pyridazinones were synthesized rationally by this methodology as full-color tunable fluorescent agents (426–612 nm). The

**Keywords:** arylation • cell imaging • copper • cross-coupling • fluorescent dyes

N2 position of pyridazinones was modified by different aryl group such as benzothiazole, *N,N*-dimethylaniline, 3-quinoline, 4-isoquinoline and 2-thiophene, resulting in a series of full-color tunable fluorescent reagents. Meanwhile, the effects of electron-donating and electron-withdrawing groups of the 6-substituted phenyl ring have also been investigated to optimize the fluorescent properties. These fluorescent core frameworks were studied in several cell lines as fluorescent dyes. Different colors from blue to red were observed by using fluorescence microscopy and confocal microscopy.

## Introduction

Fluorescent organic materials have attracted considerable attention due to their potential uses in biological science, clinical diagnosis, and drug discovery.<sup>[1]</sup> Despite the rapid development of organic fluorophores, the core skeletons possessing tunable emission wavelength is quite limited, and the rational design of new fluorescent reagents with desirable photophysical properties is far from the requirement of scientific research. 4-Bora-3a,4a-diaza-*s*-indacene (BODIPY) and cyanine dyes are the well-known organic fluorophores with correlation between structures and their photophysical properties.<sup>[2]</sup> Nevertheless, their molecular

structure must be significantly changed to tune the emission wavelength, which increases the difficulty of synthesis. Another group of fluorescent materials with tunable and predictable emission wavelengths is quantum dots (QDs), which are generally composed of heavy metals such as CdSe and CdTe.<sup>[3]</sup> However, QDs are still not completely suitable for biological applications due to their innate toxicity.<sup>[4]</sup> Recently, Park and co-workers developed a full-color tunable fluorescent core skeleton, 1,2-dihydropyrrolo[3,4- $\beta$ ]indolizin-3-one, with a tunable emission wavelength ranging from 420–613 nm. After incorporating a maleimide group for bioconjugation to thiol moieties, two selected compounds proved their applicability as labeling agents for immunocytochemistry.<sup>[5]</sup>

It is well-known that chemical modification of the  $\pi$  conjugation or variations in substituents and substitution positions can influence the energy levels and/or dipole moments in the ground and excited states of the core fluorophores, which gives rise to different optical and photochemical properties of fluorescent materials.<sup>[6]</sup> Thus, to design an organic chromophore with desirable photochemical and photophysical properties, an understanding of the relationship between its molecular structure and its function is required.

Pyridazinones, as a vital type of heterocycles, have been used as a pharmacophore with versatile biological functions in the past decades (Figure 1). Recently, N-arylated pyrida-

[a] Dr. L. Liang, W. Wang, F. Xu, Dr. Y. Niu, Dr. P. Xu  
Department of Medicinal Chemistry  
School of Pharmaceutical Sciences  
Peking University Health Science Center  
Beijing 100191 (P.R. China)  
E-mail: pingxu@bjmu.edu.cn

[b] J. Wu, Dr. B. Xu  
State Key Laboratory of Natural and Biomimetic Drugs  
School of Pharmaceutical Sciences  
Peking University Health Science Center  
Beijing 100191 (P.R. China)  
E-mail: xubo@bjmu.edu.cn

Supporting information for this article is available on the WWW under <http://dx.doi.org/10.1002/chem.201302495>.

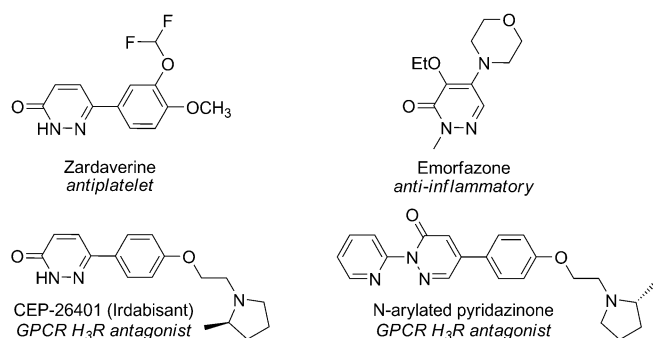


Figure 1. Bioactive compounds containing a pyridazinone scaffold.

zinsones have been developed as G-protein-coupled-receptor (GPCR) histamine 3 receptor ( $H_3R$ ) antagonists associated with several central nervous system (CNS) diseases.<sup>[7]</sup> Our original attempt for the discovery of a new core skeleton was based on extension of the conjugation system of pyridazinone, by using a transition-metal-catalyzed cross-coupling reaction. Nevertheless, the traditional synthetic method of these pyridazinones suffered from several drawbacks, such as a tedious procedure, hazardous solvents, and narrow tolerance of the substrates.<sup>[8]</sup> Furthermore, an efficient, economical, and environmentally friendly procedure for the N-functionalization of pyridazinones in aqueous phase has not been fully developed. Given that both pyridazinone and organic halide substrates are insoluble in water, resulting in poor reactivity, the application of an aqueous strategy for the C–N cross-coupling reaction has long been lacking in development. In the past decades, DMF and some other organic solvents represent the most widely used solvents, which is commonly adopted in catalysis of CuI with  $CS_2CO_3$  as a base.<sup>[9]</sup> If this reaction could be transferred into water, it would provide us abundant opportunities in the combinatorial synthesis of a diversity-oriented fluorescence library without tedious work-ups and hazardous residual.

On the other hand, an increasing interest in developing aqueous catalysis has emerged as important alternative strategies for the traditional procedures carried out in organic solvents.<sup>[10]</sup> According to the major principles of green chemistry, water is the ideal solvent due to the fact that it is abundant, nontoxic, and nonflammable.<sup>[11]</sup> In a recent survey, most pharmaceutical companies are considering water as a potential solvent.<sup>[12]</sup> So far, tremendous efforts have been made to switch organic reactions to water, among those cases, copper-catalyzed cross-coupling reaction is an excellent example; this is one of the most powerful tools for the construction of C–N bonds.<sup>[13]</sup> In terms of the copper catalysts, water-soluble copper–salen complexes were widely used in aqueous catalysis such as Ullmann reactions,<sup>[14]</sup> and azide–alkyne cycloadditions (CuAAC).<sup>[15]</sup> However, most attention has been paid to the salicylaldehyde moieties that are easily modified by hydrophilic groups, making the entire complex soluble in water. On the contrary, the diamine moiety has long been neglected despite subtle variations of this component may influence the property and reactivity of

the catalyst.<sup>[16]</sup> As we know, rational screening of the diamine moiety has not been achieved, thus the depth of information of this type of catalyst is still ambiguous.

In spite of an increasing number of relevant reports, the use of transition-metal-catalyzed N-arylation of heteroarenes to discover new full-color tunable fluorescent core frameworks still remains less explored. Therefore, to achieve the construction of C–N bond of pyridazinones in aqueous environment and also to overcome the disadvantages of traditional methods, herein we report a copper-catalyzed cross-coupling reaction of pyridazin-3(2H)-ones with organic halides, based on our rational screening of the copper–salen complexes as catalyst. The N-arylated products with diverse colors were further applied as fluorescent dyes in cell imaging.

## Results and Discussion

Recently, we reported a relay catalysis by copper catalysis in a tandem dehydrogenation/dechlorination sequence, which was successfully applied in the synthesis and medicinal study of pyridazinones.<sup>[17]</sup> We found that the electronic property of substituents at the N2 position of pyridazinones was important for the photophysical properties. To facilitate the aqueous synthesis of these compounds, a series of copper–salen complexes **Cu1**–**Cu14** were designed and the structures are shown in Figure 2.

**Screening, optimization, and evolution of the copper–salen catalysts in the cross-coupling reaction:** Initially, we chose the cross-coupling reaction of 3'-chloro-6-phenylpyridazin-3(2H)-one with bromobenzene for screening the catalysts. The structure of the copper–salen complexes are shown in Figure 2 and the results are summarized in Figure 3. We investigated different modifications of either the diamine or salicylaldehyde moiety of the original copper–salen complex **Cu1**, which exhibited negligible reactivity in water. First, we equipped the diamine with carboxylic or phenoxyacetic acid group(s); the yields of the desired cross-coupling product were evidently increased (Figure 3; **Cu2** and **Cu3**). Then, we studied the modification of the salicylaldehydes by hydroxyl or sulfonate groups, which resulted in quite different yields (Figure 3; **Cu4** and **Cu5**). As expected, when the salicylaldehyde moieties were substituted by hydrophilic group such as sulfonate, the solubility of the copper complex was remarkably improved and its performance in the cross-coupling reaction was promoted considerably (Figure 3; **Cu5**). Additionally, we also proved that hydroxyl group could improve the solubility and then enhanced the reactivity slightly (Figure 3; **Cu4**). With confirmation of the sulfonate-modified salicylaldehyde as one half part of the ligand, we continued to study the other half part of the Schiff base ligand using 1,2-diaminocyclohexane and ethylenediamine. As shown in Figure 3, both catalysts gave considerably improved results (**Cu6** and **Cu8**). To confirm the importance of the N,N,O,O tetra-coordinated ligand, a half-condensed

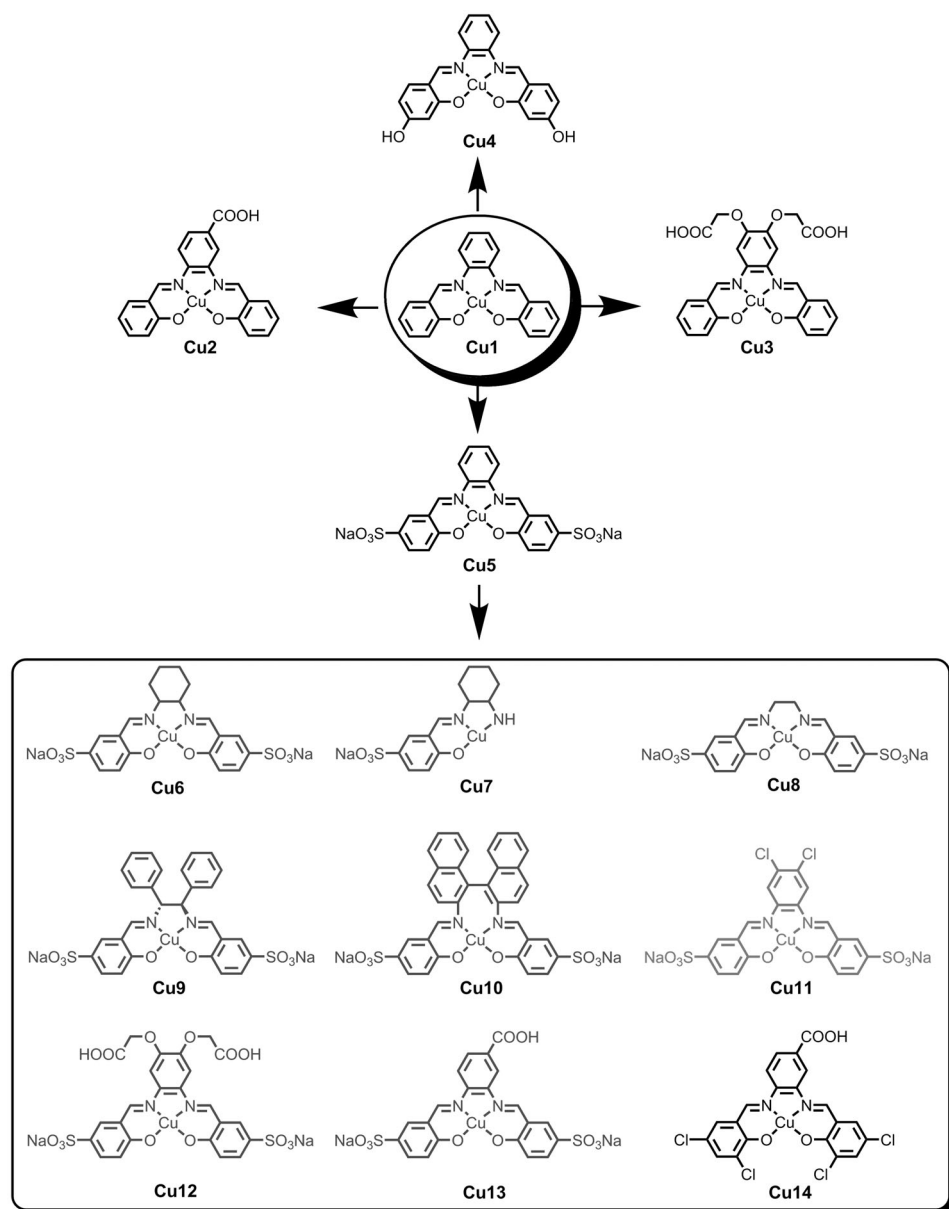


Figure 2. Copper-salen complexes used as catalysts.

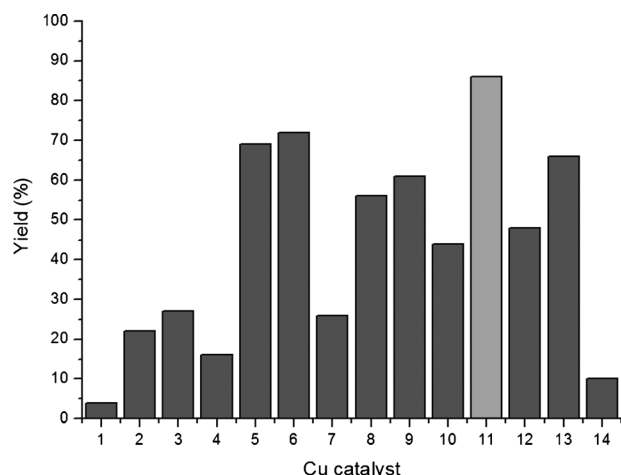


Figure 3. Yields obtained by various copper complexes.

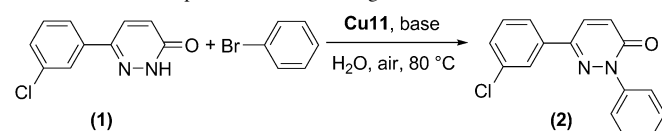
Schiff base ligand was synthesized and employed in the cross-coupling reaction. As expected, the reactivity of **Cu7** decreased dramatically, probably due to its poor solubility and stability in water.

To further optimize the structure of the catalyst and improve the cross-coupling reaction, we hypothesized that suitable enhancement of the lipophilicity of the diamine moiety might increase the affinity between the catalyst and lipophilic substrates. We delicately tuned the balance between the hydrophobic and hydrophilic property of the catalyst by using a variety of diamines including 1,2-diphenyl ethylenediamine, 1,1'-binaphthyldiamine, 4,5-dichlorobenzene-1,2-diamine, 2,2'-((4,5-diamino-1,2-phenylene)bis-(oxy))diacetic acid, and 3,4-diaminobenzoic acid to modify the upper-half of the ligand. As expected, **Cu11** bearing dichloro groups showed the highest reactivity (Figure 3). However, bulky groups on the diamines such as 1,2-diphenyl and binaphthyl showed a negative effect (Figure 3; **Cu9** and **Cu10**), as did hydrophilic groups such as phenoxyacetic acid and carboxylic acid (**Cu12** and **Cu13**). Compared with **Cu13**, if the sulfonate groups of salicylaldehyde were replaced by a hydrophobic group such as chloro, the reactivity was evidently decreased (Figure 3;

**Cu14**). By design, the upper-half moiety of **Cu11** is lipophilic, and affinitive to the organic substrates, whereas the lower-half moiety is fully soluble in water, which facilitates the reaction compatibility in water. Therefore, the potent reactivity of **Cu11** is attributed to its oil/water amphoteric property derived from the two halves of the ligand.

**Screening of the optimized reaction conditions for Cu11 as the catalyst in the cross-coupling reaction:** After the screening of catalyst, the inorganic and organic bases including  $\text{Na}_2\text{CO}_3$ ,  $\text{Cs}_2\text{CO}_3$ ,  $\text{K}_2\text{CO}_3$ ,  $\text{K}_3\text{PO}_4$ ,  $\text{NaOH}$ ,  $\text{KOH}$ , and triethylamine were investigated, in which  $\text{Na}_2\text{CO}_3$  was found to be the optimal choice (Table 1, entries 1–7). Moreover, the catalytic system showed low reactivity in organic solvent such

Table 1. Selected representative screening of the reaction.<sup>[a]</sup>



Entry	Catalyst	Base	Yield [%] <sup>[b]</sup>
1	<b>Cu11</b>	Na <sub>2</sub> CO <sub>3</sub>	86
2	<b>Cu11</b>	K <sub>2</sub> CO <sub>3</sub>	77
3	<b>Cu11</b>	CS <sub>3</sub> CO <sub>3</sub>	79
4	<b>Cu11</b>	K <sub>3</sub> PO <sub>4</sub>	75
5	<b>Cu11</b>	NaOH	64
6	<b>Cu11</b>	KOH	50
7	<b>Cu11</b>	Et <sub>3</sub> N	trace
8	<b>Cu11</b>	Na <sub>2</sub> CO <sub>3</sub>	26 <sup>[e]</sup>
9	<b>Cu11</b>	Na <sub>2</sub> CO <sub>3</sub>	30 <sup>[d]</sup>
10	<b>Cu11</b>	Na <sub>2</sub> CO <sub>3</sub>	82 <sup>[e]</sup>
11	<b>Cu11</b>	Na <sub>2</sub> CO <sub>3</sub>	52 <sup>[f]</sup>
12	<b>Cu11</b>	Na <sub>2</sub> CO <sub>3</sub>	84 <sup>[g]</sup>
13		Na <sub>2</sub> CO <sub>3</sub>	0
14	<b>Cu11</b>		0

[a] 3'-Chloro-6-phenylpyridazinone (1.0 mmol), bromobenzene (1.1 mmol), **Cu11** (5 mol %), base (2.0 mmol), in H<sub>2</sub>O at 80 °C for 12 h. [b] Yield of the isolated product. [c] DMF as solvent. [d] O<sub>2</sub> atmosphere. [e] N<sub>2</sub> atmosphere. [f] T = 60 °C. [g] T = 100 °C.

as DMF (26 %, Table 1, entry 8). Under different gas atmosphere, lower yields were detected especially in the oxygen atmosphere (Table 1, entries 9 and 10). As we expected, a lower temperature resulted in a lower yield (52 %, Table 1, entry 11). Increasing the temperature to 100 °C also gave a slight decreased yield (Table 1, entry 12).

#### Application of the catalytic system to the cross-coupling reaction between various pyridazinones and organic halides:

With the optimized conditions in hand, we studied the generality of the reactions between different aryl/alkyl halides and 3'-chloro-6-phenylpyridazin-3(2H)-one. Various aryl halides bearing either electron-donating or electron-withdrawing groups converted to the desired products in modest to excellent yields and the results are listed in Table 2. For example, the *para*-substituted aryl bromide substrates bearing –NO<sub>2</sub>, –CF<sub>3</sub>, –CN, –Cl, and –F groups afforded excellent yields. Electron-donating group (methoxyl and methyl)-substituted substrates showed slightly lower yields (Table 2, 81 and 71 %, respectively). The *meta*-substituted aryl bromide substrates also exhibited good yields. Similarly, substrates bearing electron-withdrawing groups showed higher yields than those bearing electron-donating groups. In this group, 3-bromobenzonitrile resulted in the highest yield (88 %). 3-bromonitrobenzene and 1-bromo-3-chlorobenzene afforded high yields (80 and 86 %, respectively). 3-bromotoluene and 3-bromoanisole afforded modest yields (74 and 66 %, respectively). The *ortho*-substituted aryl bromides showed remarkably lower yields, probably due to the steric effect. 2-bromonitrobenzene and 1-bromo-2-chlorobenzene afforded modest yields (70 and 71 %, respectively). 1-bromo-2-fluorobenzene and 2-bromotoluene gave lower

yields (64 and 60 %, respectively). Furthermore, disubstituted aryl bromides bearing –CF<sub>3</sub>, –Cl, and –CH<sub>3</sub> groups also gave good yields. In addition, other aryl halides including 2-bromonaphthalene, 6-bromo-1,4-benzodioxane, and 1-bromopentafluorobenzene gave good to modest yields (85, 56, and 67 %, respectively). Alkyl bromides including cyclopentyl bromide and cyclohexyl bromide were also employed in this reaction and modest yields were obtained (65, 72 %, respectively). It is noteworthy that most of the solid products could be separated from the aqueous mixture with high purity through filtration and washing, which simplifies the traditional procedures.

To expand the scope of pyridazinones, we applied this catalytic system to a variety of pyridazinone substrates. To our delight, most of the substrates afforded the desired products with good to excellent yields. As shown in Table 3, 6-phenylpyridazin-3(2H)-one was used with bromobenzene and 1,4-dibromobenzene in the cross-coupling reaction to give the products in excellent yields (95 and 86 %, respectively). Mono-chloro and dichloro-substituted substrates also exhibited good yields. For example, both 4'-chloro-6-phenylpyridazin-3(2H)-one and 2'-chloro-6-phenylpyridazin-3(2H)-one afforded the N-arylated products in high yields above 85 %. 2',4'-dichloro-6-phenylpyridazinone was also used to the reaction with bromobenzene and 89 % yield was obtained. We further investigated the reaction of 2',4'-dichloro-6-phenylpyridazinone and 1,4-dibromobenzene with a molar ratio 2.1:1.0 and the dimer product was obtained with 82 % yield. Other pyridazinones without 6-phenyl group were also examined. For instance, when the 6-phenyl group was replaced by –Cl, the cross-coupling reaction also proceeded with high yield (83 %). 4-bromophthalazin-1(2H)-one was also used to give the product in 78 % yield.

**Rational design and study of N-substituted 6-phenylpyridazinones as fluorescent reagents:** With the optimized reaction conditions in hand, a series of pyridazinones and organic halides were applied in this reaction and the results are listed in Table 4. In general, all of the substrates afforded the N-arylation products (**PyL1–PyL8**) with moderate to excellent yields ranging from 60 to 84 %. With the compilation of these fluorescent compounds, we evaluated the photophysical and photochemical properties of each individual fluorophore. As shown in Figure 4a, the overlaid fluorescent emission spectra highlight the accomplishment of full-color tunable emissive fluorophores based on the 6-phenyl pyridazinone skeleton. As expected, a dramatic change in the fluorescence properties can be achieved successfully within a single molecular framework simply by changing the substituents at only two variation points in the fluorophore. The direct comparison of the electronic properties of the R<sup>1</sup> substituents clearly demonstrates the tunability of this core skeleton. The maximum emission wavelengths are increased in the following order: R<sup>1</sup> = phenyl (the model N-arylation product), 4-isoquinoline (**PyL7**), 3-quinoline (**PyL6**), 2-benzothiazole (**PyL4**), 4-methoxyphenyl (**2ag**), 2-thiophenyl (**PyL8**), 4-dimethylamino phenyl (**PyL1**) on a single skele-



Table 2. Reaction of various organic halides with 3'-chloro-6-phenylpyridazin-3(2H)-one under the optimized conditions.<sup>[a]</sup>

1	2	Yield [%]	1	2	Yield [%]	1	2	Yield [%]	
R =			R =			R =			
NO <sub>2</sub>	<b>2aa</b>	89	NO <sub>2</sub>	<b>2ah</b>	80	NO <sub>2</sub>	<b>2am</b>	70	
CF <sub>3</sub>	<b>2ab</b>	90	CN	<b>2ai</b>	88	Cl	<b>2an</b>	71	
CN	<b>2ac</b>	92	Cl	<b>2aj</b>	86	F	<b>2ao</b>	64	
Cl	<b>2ad</b>	90	CH <sub>3</sub>	<b>2ak</b>	74	CH <sub>3</sub>	<b>2ap</b>	60	
F	<b>2ae</b>	87	OMe	<b>2al</b>	66				
CH <sub>3</sub>	<b>2af</b>	81							
OMe	<b>2ag</b>	71							
R =			<b>2at</b>	85	<b>2au</b>	56			
CF <sub>3</sub>	<b>2aq</b>	84							
Cl	<b>2ar</b>	86							
CH <sub>3</sub>	<b>2as</b>	70							
	<b>2av</b>	67	<b>2aw</b>	65	<b>2ax</b>	72			

[a] 3'-Chloro-6-phenylpyridazinone (1.0 mmol), bromobenzene (1.1 mmol), **Cu11** (5 mol %), Na<sub>2</sub>CO<sub>3</sub> (2.0 mmol), in H<sub>2</sub>O at 80 °C for 12 h.

ton with fixed R<sup>2</sup> substituent such as *meta*-Cl group. The corresponding emission wavelengths of **PyL**<sub>7</sub>, **PyL**<sub>6</sub>, **PyL**<sub>4</sub>, **2ag**, **PyL**<sub>8</sub>, and **PyL**<sub>1</sub> are 426, 458, 478, 501, 517 and 612 nm, respectively. Fine tuning of the fluorescent property of **PyL** compounds is feasible by changing the R<sup>2</sup> group but keeping a fixed R<sup>1</sup> substituent. For instance, the electron-donating group on the 6-phenyl ring blueshifts the emission peak, which was achieved by our further modification of the structures of **PyL**s. As shown in Table 4, **PyL**<sub>1</sub> showed a dramatic increase of fluorescence with large bathochromic shift to 612 nm. When the 6-phenyl group was substituted by electron-donating *ortho*-ethoxy group, the fluorescent emission of **PyL**<sub>2</sub> could be tuned slightly with a hypochromatic shift to 597 nm. Further study of structure–activity relationship (SAR) showed the 6-phenyl group is indispensable for the whole conjugated system of fluorescent core framework. For example, when the 6-phenyl group is replaced by a chloro group, the fluorescent intensity of **PyL**<sub>3</sub> decreased severely (Figure 4c, ii). Besides the phenyl groups, we also investigated the effect of other aromatic groups on the N2 position of pyridazinones. For instance, 2-bromobenzo[d]thia-

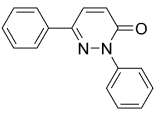
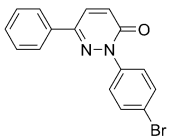
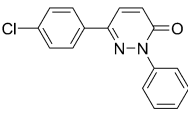
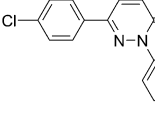
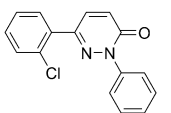
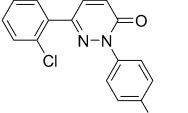
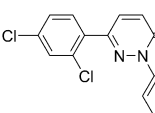
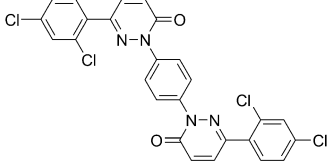
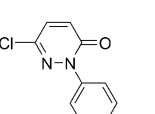
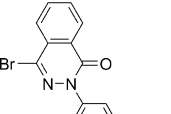
zole was used as the organic halide for the cross-coupling reaction, which afforded modest yields (**PyL**<sub>4</sub> and **PyL**<sub>5</sub>). Compared with **PyL**<sub>5</sub>, which has a non-substituted 6-phenyl group, the emission of **PyL**<sub>4</sub> showed a blueshift to 478 nm when the *meta*-position was substituted by chloro group (Figure 4c, i). Meanwhile, the fluorescent intensity of **PyL**<sub>4</sub> was increased to 0.25 compared with **PyL**<sub>5</sub> (0.19). Moreover, quinoline (**PyL**<sub>6</sub>) and isoquinoline (**PyL**<sub>7</sub>) were also independently investigated as donors to study the photophysical properties. As shown in Figure 4c, iii, **PyL**<sub>7</sub> displayed negligible fluorescence compared with **PyL**<sub>6</sub>. Thiophene, which was widely used in optical materials and devices, was also employed in the cross-coupling reaction with 3'-chloro-6-phenylpyridazinone and green fluorescence was obtained (**PyL**<sub>8</sub>).

#### Application of the N-arylated pyridazinones in cell imaging by using fluorescent and confocal microscopy:

Molecular fluorescent-imaging techniques are helpful to understand biological processes at the molecular level

(e.g., intracellular pH indicators,<sup>[18]</sup> sensors for reactive oxygen and nitrogen species,<sup>[19]</sup> metal sensors,<sup>[20]</sup> diagnosis imaging tools<sup>[21]</sup>) and mechanisms.<sup>[22]</sup> Thus, the development of new fluorescent bioimaging probes still remains an attractive and promising goal.<sup>[23]</sup> To demonstrate the use of **PyL**s as dye stains for cell imaging, their chemo- and photostability, as well as the cytotoxicity or cell viability, were assessed first. The pH-dependent absorption and emission spectra of **PyL**<sub>2</sub>, **PyL**<sub>3</sub>, **PyL**<sub>6</sub>, and **PyL**<sub>8</sub> in the solution of the mixed buffers (NaOAc, Mes, Mops, and Tris) and DMSO (0.5 %, V<sub>DMSO</sub>/V<sub>buffer</sub>) were measured and shown in Figure S1 (see the Supporting Information). Among our new fluorophores, we chose **PyL**<sub>8</sub> for direct comparison with the well-known fluorescent molecule fluorescein.<sup>[24]</sup> As a result, **PyL**<sub>8</sub> is more resistant to photobleaching than fluorescein (see Figure S2 in the Supporting Information). Fluorescein is well-known to have multiple ionization equilibria, which leads to pH-dependent absorption and emission. Unlike fluorescein, because of its new molecular framework, the fluorescence intensity and maximum emission wavelength of **PyL**<sub>8</sub> are not influenced by pH value in the range 4–9 (physiological

Table 3. Reaction of organic halides with various pyridazin-3(2*H*)-one under the optimized conditions.<sup>[a]</sup>

		
<b>2ba</b> 95 %	<b>2bb</b> 86 %	<b>2bc</b> 92 %
		
<b>2bd</b> 85 %	<b>2be</b> 88 %	<b>2bf</b> 87 %
		
<b>2bg</b> 89 %	<b>2bh</b> 82 % <sup>[b]</sup>	
		
<b>2bi</b> 83 %	<b>2bj</b> 78 %	

[a] Pyridazinone (1.0 mmol), bromobenzene (1.1 mmol), **CuII** (5 mol %), Na<sub>2</sub>CO<sub>3</sub> (2.0 mmol), in H<sub>2</sub>O at 80 °C for 12 h. [b] Molar ratio of pyridazinone/1,4-dibromobenzene = 2.1:1.0.

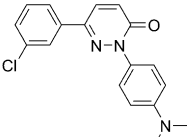
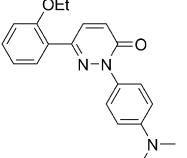
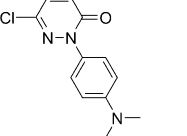
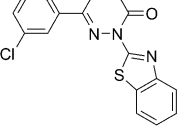
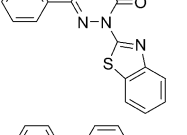
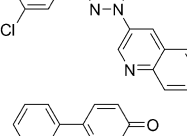
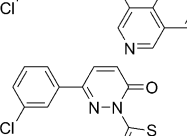
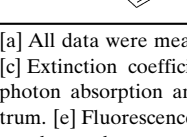
range of in vivo system), which is an important element in bioimaging and bioapplication.<sup>[25]</sup> Above all, it indicated that these PyL compounds 1) were stable over the pH ranges (4–9), and 2) are more resistant to photobleaching than fluorescein.

Cell viability assays in four cell lines including MCF-7, DU-145, HeLa, and SW480 were conducted by using the 3-(4,5-diethyl-2-thiazolyl)-2,5-diphenyl tetrazolium bromide (MTT >) assay. The cell viability data after treatment with 100 μM of the pyridazinone products and PyLs for 24 and 48 h are shown in Table S1 in the Supporting Information. Although the growth inhibition rates of **PyL7** were 67.4 and 75.0 % in SW480 cells for treatment at 24 and 48 h, respectively, other compounds are virtually nontoxic over a period of 24 to 48 h (see Table S1 in the Supporting Information).

To further explore the practical application of these new fluorescent molecules, the MCF-7 cells were incubated with a series of PyLs. As shown in Figure 5, PyLs showed potent cell permeability and successfully marked MCF-7 cells, and preferentially accumulated in the cytoplasm, suggesting that this class of membrane-permeable fluorophores (PyLs) could be potentially useful reagents for biological imaging.

To further explore the application of PyLs in living cell imaging, we observed the cell-imaging experiment by using confocal microscopy. The confocal microscopy images showed that **PyL2** could be taken up efficiently by HeLa cells and the optimum concentrations are 10 μM. As shown

Table 4. Photophysical data of PyL compounds in DMSO.<sup>[a]</sup>

Structure	PyLn	Yield <sup>[b]</sup> [%]	$\epsilon_{\max}$ <sup>[c]</sup>	$\lambda_{\text{ex}}/\lambda_{\text{em}}$ <sup>[d]</sup>	$\Phi$ <sup>[e]</sup>
	<b>PyL1</b>	69	0.54	382, 612	0.082
	<b>PyL2</b>	66	0.61	375, 597	0.095
	<b>PyL3</b>	72	0.56	304, 603	n.d. <sup>[f]</sup>
	<b>PyL4</b>	60	1.29	363, 478	0.25
	<b>PyL5</b>	84	1.42	366, 489	0.19
	<b>PyL6</b>	78	0.94	304, 458	0.064
	<b>PyL7</b>	70	0.60	304, 426	n.d.
	<b>PyL8</b>	68	1.02	381, 517	0.077

[a] All data were measured in DMSO. [b] Yields of the isolated products. [c] Extinction coefficient in  $1 \times 10^4 \text{ M}^{-1} \text{ cm}^{-1}$ . [d]  $\lambda_{\max}$  values of the one-photon absorption and emission spectra in nm of the absorption spectrum. [e] Fluorescence quantum yield, the uncertainty is  $\pm 15\%$ . [f] n.d. = not detected.

in Figure 6, we selected fluorescent images of HeLa cells incubated with **PyL2** (10 μM, 0.5 h) as a marker. In particular, **PyL2** displayed punctate luminescence in the cytoplasm.

## Conclusion

A highly efficient and “green” protocol has been developed for the synthesis of N-functionalized pyridazinones. The catalytic system consists of a water-soluble copper–salen complex, which is endowed with reasonable balance of hydro-

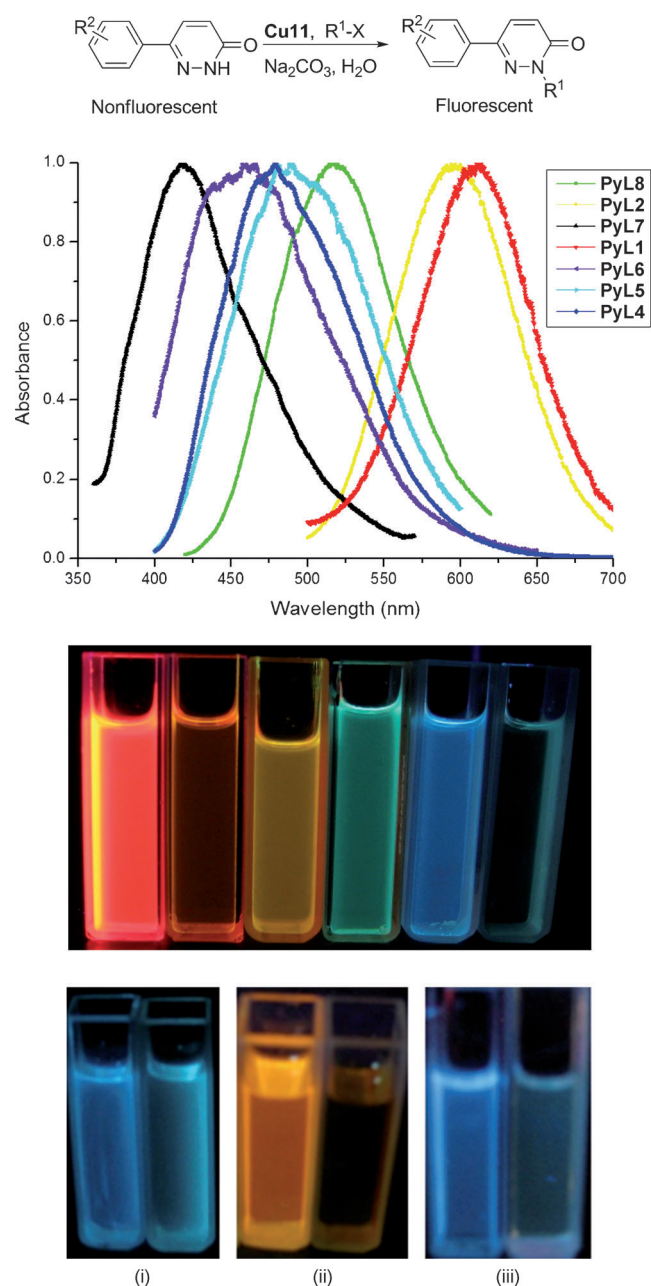


Figure 4. a) Synthesis and normalized emission spectra of **PyL1**, **PyL2**, and **PyL4–PyL8** ( $\approx 2.0 \mu\text{m}$ ) in DMSO. b) Selected fluorescence images of PyLs in DMSO, irradiated at 365 nm. From left to right: **PyL1**, **PyL3**, **PyL2**, **PyL8**, **PyL4**, and **PyL7**. c) Compared fluorescence of i) **PyL4** versus **PyL5**, ii) **PyL2** versus **PyL3**, and iii) **PyL6** versus **PyL7**.

philic and hydrophobic properties. More importantly, this reaction can be simply achieved in water and in an air atmosphere. Following this protocol, a full-color tunable fluorescent core skeleton have been developed based on N-arylated 6-phenylpyridazin-3(2H)-ones. This core skeleton can accommodate various emission maxima simply by changing substituents at the N2 and 6-phenyl positions, having different electronic properties. These new fluorophores have excellent photophysical and photochemical properties, resistance to photobleaching, moderate-to-considerable quantum

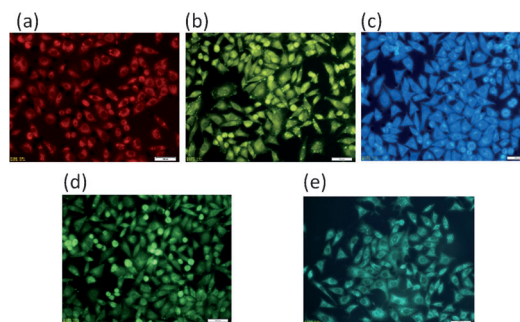


Figure 5. Selected fluorescence images of MCF-7 cells incubated with 100  $\mu\text{M}$  of a) **PyL1**, b) **PyL2**, c) **PyL4**, d) **PyL8**, e) **PyL5**.

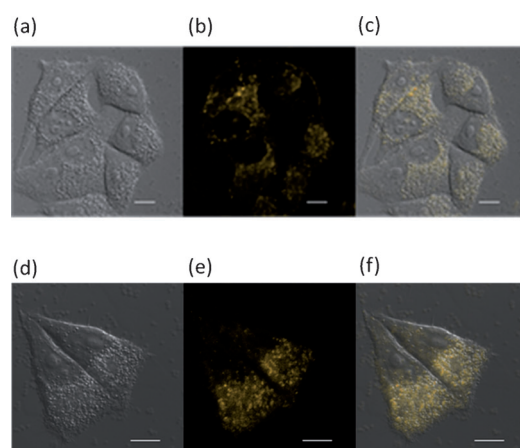


Figure 6. a) and d) Bright-field images of the HeLa cells stained with **PyL2**; b) and e) one-photon microscopy image of the same cells with excitation at 488 nm; c) and f) merged image. Scale bar: 10  $\mu\text{m}$ .

yields, pH-independent fluorescence, large Stokes shifts, and drug-like lipophilicity for membrane permeability. The fluorophores have successfully marked MCF-7 and HeLa cells, exhibiting their future potential as useful bioimaging fluorescence probes. Further applications of these fluorophores in biological imaging are currently being studied.

## Experimental Section

**General:** All reagents unless otherwise stated were purchased from commercial suppliers and used without further purification. <sup>1</sup>H, <sup>13</sup>C and <sup>19</sup>F NMR spectra were recorded on Bruker AVIII-400 spectrometers with [D<sub>6</sub>]DMSO or CDCl<sub>3</sub> as solvent. Chemical shifts are reported in ppm using TMS as internal standard. Mass spectra (MS) and high-resolution mass spectra (HRMS) were recorded with a Finnigan MAT 95 spectrometer (EI) with an ionization potential of 70 eV. Infrared spectra (IR) were recorded with a Bruker Tensor 27 spectrometer. Absorption bands are reported in wave numbers (cm<sup>-1</sup>). For flash chromatography, silica gel from Merck (200–300 mesh) was used. Merck silica gel GF<sub>254</sub> plates were used for TLC. The substances were detected with UV light (254 nm) and iodine. Substances that have already been reported in the literature were identified by comparison of the obtained <sup>1</sup>H and <sup>13</sup>C NMR spectra with those reported in the literature. New substances were fully characterized by infrared (IR), <sup>1</sup>H, <sup>13</sup>C, <sup>19</sup>F NMR (products

consisting of fluoride) and mass spectrometry (MS). Additional characterization data were obtained by high-resolution mass spectrometry (HRMS).

All cells were incubated in complete medium (Dulbecco's modified Eagle's medium, DMEM, supplemented with 10% fetal bovine serum (FBS), 1% penicillin-streptomycin) at 37°C in an atmosphere containing 5% CO<sub>2</sub>. The steady-state absorption spectra were obtained with an Agilent 8453 UV/Vis spectrophotometer in 10 mm path length quartz cuvettes with a dye concentration of  $\approx 1 \times 10^{-5}$  M. Single-photon luminescence spectra were recorded by using an Edinburgh Instrument FLS920 Combined Fluorescence Lifetime and Steady-state spectrophotometer. All measurements were performed at room temperature).

**General procedure for the screening of the copper(II)–salen complexes as catalysts:** 3'-chloro-6-phenylpyridazinone (206 mg, 1.0 mmol), bromobenzene (173 mg, 1.1 mmol), and Na<sub>2</sub>CO<sub>3</sub> (312 mg, 2.0 mmol) were added to a stirred mixture of the copper–salen complex (0.05 mmol) in water (2 mL) at room temperature. The tube was then sealed and the temperature was increased to 80°C in the air for 12 h. The reaction mixture was filtered and the solid residue was purified by washing with distilled water (10 mL  $\times$  3) to remove the residual of catalyst and base; and *n*-hexane (2 mL  $\times$  3) to remove the excessive organic residuals with spectrum purity. For further purification, the products could be purified by column chromatography on silica gel using mixtures of *n*-hexane ether and ethyl acetate (2:1) as the eluent.

**General procedure for the reactions shown in Table 1:** 3'-chloro-6-phenylpyridazinone (206 mg, 1.0 mmol), bromobenzene (173 mg, 1.1 mmol), and base (2.0 mmol) were added to a stirred mixture of **Cu11** (32.5 mg, 0.05 mmol) in water (2 mL) at room temperature. The tube was then sealed and the temperature was increased to 80°C in the air. On completion of the reaction (as monitored by TLC) for 12 h, reaction mixture was filtrated and the solid residue was purified by washing with distilled water (10 mL  $\times$  3) to remove the residual of catalyst and base; and *n*-hexane (2 mL  $\times$  3) to remove the excessive organic residuals with spectrum purity. For further purification, the products could be purified by column chromatography on silica gel using mixtures of *n*-hexane ether and ethyl acetate (2:1) as the eluent.

**General procedure for the reactions shown in Table 2:** 3'-chloro-6-phenylpyridazinone (206 mg, 1.0 mmol), organic halide (1.1 mmol), and Na<sub>2</sub>CO<sub>3</sub> (312 mg, 2.0 mmol) were added to a stirred solution of **Cu11** (32.5 mg, 0.05 mmol) in water (2 mL) at room temperature. The tube was then sealed and the temperature was increased to 80°C in the air. On completion of the reaction for 12 h, reaction mixture was filtrated and the solid residue was purified by washing with distilled water (10 mL  $\times$  3) and *n*-hexane (2 mL  $\times$  3) with spectrum purity. For further purification, the products were purified by column chromatography on silica gel using mixtures of *n*-hexane and ethyl acetate (2:1) as the eluent.

**General procedure for the reactions shown in Table 3:** Pyridazinone (1.0 mmol), bromobenzene (1.1 mmol) or 1,4-dibromobenzene (0.5 mmol), and Na<sub>2</sub>CO<sub>3</sub> (312 mg, 2.0 mmol) were added to a stirred solution of **Cu11** (32.5 mg, 0.05 mmol) in water (2 mL) at room temperature. The tube was then sealed and the temperature was increased to 80°C in the air. On completion of the reaction for 12 h, reaction mixture was filtrated and the solid residue was purified by washing with distilled water (10 mL  $\times$  3) and *n*-hexane (2 mL  $\times$  3) with spectrum purity. For further purification, the products were purified by column chromatography on silica gel using mixtures of *n*-hexane and ethyl acetate (2:1) as the eluent.

**General procedure for the synthesis of PyLs shown in Table 4:** Pyridazinone (1.0 mmol), organic halide (1.1 mmol), and Na<sub>2</sub>CO<sub>3</sub> (312 mg, 2.0 mmol) were added to a stirred solution of **Cu11** (32.5 mg, 0.05 mmol) in water (2 mL) at room temperature. The tube was then sealed and the temperature was increased to 80°C in the air. On completion of the reaction for 12 h, reaction mixture was filtrated and the solid residue was purified by washing with distilled water (10 mL  $\times$  3) and *n*-hexane (2 mL  $\times$  3) with spectrum purity. For further purification, the products were purified by column chromatography on silica gel using mixtures of *n*-hexane and ethyl acetate (2:1) as the eluent.

## Acknowledgements

This work was supported by the National Natural Science Foundation of China (21202003/21172012), the National Basic Research Program of China (2012CB518000) and the Beijing Natural Science Foundation (Design, synthesis and optimization of proteasome inhibitors as novel antitumor agents, 7112088).

- [1] a) *Applied Fluorescence in Chemistry, Biology, and Medicine*, (Eds.: W. Rettig, B. Strehmel, S. Schrader, H. Seifert), Springer: New York, **1999**; b) J. J. Lavigne, E. V. Anslyn, *Angew. Chem.* **2001**, *113*, 3212–3225; *Angew. Chem. Int. Ed.* **2001**, *40*, 3118–3130; c) J. Rao, A. Dragulescu-Andrasi, H. Yao, *Curr. Opin. Biotechnol.* **2007**, *18*, 17–25; d) J. Zhang, R. E. Campbell, A. Y. Ting, R. Y. Tsien, *Nat. Immunol. Nat. Rev. Mol. Cell. Biol.* **2002**, *3*, 906–918.
- [2] A. P. Demchenko, in *Advanced Fluorescence Reporters in Chemistry and Biology I*, Springer-Verlag: Berlin, Heidelberg, **2010**; Chapter 2.5, pp. 149–186.
- [3] a) M. Bruchez Jr., M. Moronne, P. Gin, S. Weiss, A. P. Alivisatos, *Science* **1998**, *281*, 2013–2016; b) C. B. Murray, D. J. Norris, M. G. Bawendi, *J. Am. Chem. Soc.* **1993**, *115*, 8706–8715; c) Z. A. Peng, X. Peng, *J. Am. Chem. Soc.* **2001**, *123*, 183–184; d) Z. A. Peng, X. Peng, *J. Am. Chem. Soc.* **2002**, *124*, 3343–3353.
- [4] R. Hardman, *Environ. Health Perspect.* **2006**, *114*, 165–172.
- [5] a) E. Kim, M. Koh, J. Ryu, S. B. Park, *J. Am. Chem. Soc.* **2008**, *130*, 12206–12207; b) E. Kim, M. Koh, B. J. Lim, S. B. Park, *J. Am. Chem. Soc.* **2011**, *133*, 6642–6649.
- [6] a) C. L. Li, S. J. Shieh, S. C. Lin, R. S. Liu, *Org. Lett.* **2003**, *5*, 1131–1134; b) Y. Yamaguchi, T. Ochi, T. Wakamiya, Y. Matsubara, Z. Yoshida, *Org. Lett.* **2006**, *8*, 717–720; c) U. Nagata, U. Chujo, *Macromolecules* **2008**, *41*, 2809–2813; d) G. Q. Zhang, S. E. Kooi, J. N. Demas, C. L. Fraser, *Adv. Mater.* **2008**, *20*, 2099–2104; e) #. Itami, K. D. Yamazaki, J. Yoshida, *J. Am. Chem. Soc.* **2004**, *126*, 15396–15397; f) C.-C. Chao, M.-K. Leung, Y. O. Su, K.-Y. Chiu, T.-H. Lin, S.-J. Shieh, S.-C. Lin, *J. Org. Chem.* **2005**, *70*, 4323–4331; g) Q. Peng, Y. P. Yi, Z. G. Shuai, J. S. Shao, *J. Am. Chem. Soc.* **2007**, *129*, 9333–9339; h) R. Pohl, P. Anzenbacher, *Org. Lett.* **2003**, *5*, 2769–2772; i) R. Pohl, V. A. Montes, J. Shinar, P. Anzenbacher, *J. Org. Chem.* **2004**, *69*, 1723–1725; j) Y. Qin, I. Kiburu, S. Shah, F. Jäkle, *Org. Lett.* **2006**, *8*, 5227–5230; k) J. Cornil, D. Beljonne, J. P. Calbert, J. L. Bredas, *Adv. Mater.* **2001**, *13*, 1053–1067; l) J. A. Marsden, J. J. Miller, L. D. Shirtcliff, M. M. Haley, *J. Am. Chem. Soc.* **2005**, *127*, 2464–2476; m) B. Liu, Z. Wang, N. Wu, M. Li, J. You, J. Lan, *Chem. Eur. J.* **2012**, *18*, 1599–1603.
- [7] a) M. Tao, L. D. Aimone, Z. Huang, J. Mathiasen, R. Raddatz, J. Lyons, R. Hudkins, *J. Med. Chem.* **2012**, *55*, 414–423; b) R. Hudkins, R. Raddatz, M. Tao, J. Mathiasen, L. Aimone, N. Becknell, C. Prouty, L. Knutsen, M. Yazdani, G. Moachon, M. Ator, J. Mallamo, M. Marino, E. Bacon, M. Williams, *J. Med. Chem.* **2011**, *54*, 4781–4792.
- [8] a) A. Coelho, E. Sotelo, E. Raviña, *Tetrahedron* **2003**, *59*, 2477–2484; b) A. Monge, P. Parrado, M. Font, E. Alvarez, *J. Med. Chem.* **1987**, *30*, 1029–1035; c) I. Sircar, R. Weishaar, D. Kobylarz, W. Moos, J. Bristol, *J. Med. Chem.* **1987**, *30*, 1955–1962; d) A. Akahane, H. Katayama, T. Mitsunaga, *J. Med. Chem.* **1999**, *42*, 779–783; e) D. Livermore, R. Bethell, N. Cammack, *J. Med. Chem.* **1993**, *36*, 3784–3794; f) E. Sotelo, A. Coelho, E. Ravina, *Tetrahedron Lett.* **2003**, *44*, 4459–4462.
- [9] I. P. Beletskaya, A. V. Cheprakov, *Coord. Chem. Rev.* **2004**, *248*, 2337–2364.
- [10] a) D. Rowe, *Science* **2007**, *317*, 323–324; b) J. Liu, *Science* **2010**, *328*, 50; c) C.-J. Li, *Acc. Chem. Res.* **2002**, *35*, 533–538; d) C.-J. Li, *Chem. Rev.* **2005**, *105*, 3095–3165.
- [11] a) I. Beletskaya, A. Cheprakov, in *Organic Synthesis in Water* (Ed.: P. Grieco), Blackie Academic & Professional, London, **1998**, Ch. 5, p. 141; b) C. I. Herrerías, X. Yao, Z. Li, C.-J. Li, *Chem. Rev.* **2007**, *107*, 2546–2562; c) A. Modak, J. Mondal, M. Sasidharan, A. Bhau-mik, *Green Chem.* **2011**, *13*, 1317–1331.

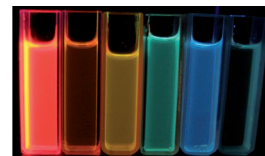
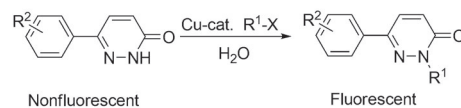



- [12] W. Watson, *Green Chem.* **2012**, *14*, 251–259.
- [13] I. Beletskaya, A. Cheprakov, in *Handbook of Organopalladium Chemistry for Organic Synthesis*, Vol. 2 (Eds.: E.-I. Negishi and A. de Meijere), Wiley, New York, **2002**, Ch. 10, p. 2957.
- [14] a) Y. Wang, Z. Wu, L. Wang, Z. Li, X.-G. Zhou, *Chem. Eur. J.* **2009**, *15*, 8971–8974; b) L. Liang, Z. Li, X.-G. Zhou, *Org. Lett.* **2009**, *11*, 3294–3297.
- [15] Y. Cai, L. Liang, J. Zhang, H. Sun, J.-L. Zhang, *Dalton Trans.* **2013**, 42, 5390–5400.
- [16] Y. Qu, F. Ke, L. Zhou, Z. Li, H. Xiang, D. Wu, X.-G. Zhou, *Chem. Commun.* **2011**, 47, 3912–3914.
- [17] a) L. Liang, G. Yang, W. Wang, F. Xu, Y. Niu, Q. Sun, P. Xu, *Adv. Synth. Catal.* **2013**, 355, 1284–1290; b) L. Liang, G. Yang, W. Wang, F. Xu, Y. Niu, Q. Sun, P. Xu, *Org. Lett.* **2013**, *15*, 2770–2773; c) L. Liang, G. Yang, F. Xu, Y. Niu, Q. Sun, P. Xu, *Eur. J. Org. Chem.* **2013**, DOI:10.1002/ejoc.201300640.
- [18] J. Han, K. Burgess, *Chem. Rev.* **2010**, *110*, 2709–2728.
- [19] a) E. W. Miller, C. J. Chang, *Curr. Opin. Chem. Biol.* **2007**, *11*, 620–625; b) X. Chen, X. Tian, I. Shin, J. Yoon, *Chem. Soc. Rev.* **2011**, *40*, 4783–4804.
- [20] a) Z. Xu, J. Yoon, D. R. Spring, *Chem. Soc. Rev.* **2010**, *39*, 1996–2006; b) E. M. Nolan, S. J. Lippard, *Chem. Rev.* **2008**, *108*, 3443–3480.
- [21] a) H. Kobayashi, M. Ogawa, R. Alford, P. L. Choyke, Y. Urano, *Chem. Rev.* **2010**, *110*, 2620–2640; b) H. Kobayashi, P. L. Choyke, *Acc. Chem. Res.* **2011**, *44*, 83–90.
- [22] J. Wu, W. Liu, J. Ge, H. Zhang, P. Wang, *Chem. Soc. Rev.* **2011**, *40*, 3483–3495.
- [23] a) B. N. G. Giepmans, S. R. Adams, M. H. Ellisman, R. Y. Tsien, *Science* **2006**, *312*, 217–224; b) M. Vendrell, D. Zhai, J. Cheng Er, Y.-T. Chang, *Chem. Rev.* **2012**, *112*, 4391–4420; c) G. Lukinavičius, K. Umezawa, N. Olivier, A. Honigsmann, G. Yang, T. Plass, V. Mueller, L. Reymond, I. R. Corrêa Jr, Z.-G. Luo, C. Schultz, E. A. Lemke, P. Heppenstall, C. Eggeling, S. Manley, K. Johnsson, *Nat. Chem.* **2013**, *5*, 132–139; d) L. M. Wysockia, L. D. Lavis, *Curr. Opin. Chem. Biol.* **2011**, *15*, 752–759; e) E. Kim, S. B. Park, *Chem. Asian J.* **2009**, *4*, 1646–1658; f) Z. Chamas, E. Marchi, A. Modelli, Y. Fort, P. Ceroni, V. Mamane, *Eur. J. Org. Chem.* **2013**, 2316–2324.
- [24] a) W.-B. Wu, M.-L. Wang, Y.-M. Sun, W. Huang, Y.-P. Cui, C.-X. Xu, *J. Phys. Chem. Solids* **2008**, *69*, 76–82; b) M. Nakazono, S. Nanbu, A. Uesaki, R. Kuwano, M. Kashiwabara, K. Zaitzu, *Org. Lett.* **2007**, *9*, 3583–3586.
- [25] a) D. Citterio, J. Takeda, M. Kosugi, H. Hisamoto, S.-I. Sasaki, H. Komatsu, K. Suzuki, *Anal. Chem.* **2007**, *79*, 1237–1242; b) L. F. Mottram, S. Boonyarattanakalin, R. E. Kovel, B. R. Peterson, *Org. Lett.* **2007**, *9*, 581–584; c) W.-C. Sun, K. R. Gee, D. H. Klaubert, R. P. Haugland, *J. Org. Chem.* **1997**, *62*, 6469–6475.

Received: June 27, 2013  
Published online: ■ ■ ■, 2013

## Fluorescence

L. Liang, W. Wang, J. Wu, F. Xu,  
Y. Niu, B. Xu,\* P. Xu\* ..... ■■■■–■■■■



 **Rational Design, Green Synthesis, and Initial Evaluation of a Series of Full-Color Tunable Fluorescent Dyes Enabled by the Copper-Catalyzed N-Arylation of 6-Phenyl Pyridazinones and Their Application in Cell Imaging**

**Colorful cores:** A simple and efficient copper-catalyzed cross-coupling reaction for the N-functionalization of pyridazinones in neat water is reported (see figure). The N2 position of pyridazinones was modified by different aryl

groups ( $R^1$ ), such as benzothiazole, *N,N*-dimethylaniline, 3-quinoline, 4-isoquinoline, and 2-thiophene, resulting in a series of full-color tunable fluorescent reagents.